Effect of cavity length detuning on the output characteristics for the middle infrared FEL oscillator of FELiChEM *

Zhou-Yu Zhao(赵周宇) He-Ting Li(李和廷)1) Qi-Ka Jia(贾启卡)

National Synchrotron Radiation Laboratory, University of Science and Technology of China, Hefei 230029, China

Abstract: FELiChEM is an infrared free electron laser (FEL) facility currently under construction, which consists of two oscillators generating middle-infrared and far-infrared laser covering the spectral range of 2.5–200 μm. In this paper, we numerically study the output characteristics of the middle-infrared oscillator with accurate cavity length detuning. Emphasis is put on the temporal structure of the micropulse and the corresponding spectral bandwidth. Taking the radiation wavelengths of 50 μm and 5 μm as examples, we show that the output pulse duration can be tuned in the range of 1–6 ps with corresponding bandwidth of 13%–0.2% by adjusting the cavity length detuning. In addition, a special discussion on the comb structure is presented, and it is indicated that the comb structure may arise in the output optical pulse when the normalized slippage length is much smaller than unity. This work has reference value for the operation of FELiChEM and other FEL oscillators.

Keywords: free electron laser oscillator, cavity length detuning, output characteristics, comb structure

PACS: 41.60.Cr, 98.70.Lt **DOI:** 10.1088/1674-1137/41/10/108101

1 Introduction

Free electron lasers (FELs) hold great promise as a high-power light source with a tunable wavelength. Many FEL user facilities have been constructed and are being proposed worldwide, from the far infrared to the hard X-ray spectral region [1–5]. These facilities are based on different kinds of FEL schemes according to their object radiation wavelength and the demands of output properties, e.g., self-amplified spontaneous emission for hard X-ray FEL [1, 6] and seeded FEL for the extreme ultraviolet FEL [2, 7]. In the infrared (IR) and terahertz (THz) regions, oscillator FEL is one of the most important FEL schemes. Nowadays infrared FEL oscillators are built worldwide as user facilities, including CLIO in France [4, 8], FHI-FEL in Germany [9, 10], FELIX in the Netherlands [11, 12] and so on. A recently proposed scheme using a pre-bunched electron bunch train provides a way to build a compact infrared and THz source, however, its optimized working frequency region is in the range of 1–5 THz [13, 14].

A new FEL user facility named FELiChEM is currently under construction in China. It consists of two oscillators driven by one RF linac, and will be used to generate middle-infrared (2.5–50 μm) and far-infrared (40-200 μm) laser [15]. It will be a dedicated IR light source aiming at energy chemistry research, and first light is targeted for the end of 2017. The FEL output characteristics are influenced by many factors. In an FEL oscillator (FELO), detuning the cavity length is an important method to control the output characteristics of the radiation and obtain the desired pulse energy, pulse length and bandwidth [16, 17]. Considering this point, the optical cavity of FELiChEM was designed with the function of convenient and accurate cavity length detuning.

In this paper, we numerically study the output characteristics for FELiChEM with the cavity length detuning. Firstly, we briefly review the relevant theory in Section 2. Then in Section 3, we describe the FELiChEM parameters and numerically investigate the optical output characteristics with cavity length detuning. A special focus is put on the comb structure inside the optical pulse in Section 4. Finally, we summarize in the last section.

2 Brief review of relevant theory

In a FELO the optical pulse and electron beam are coupled as electrons pass through the undulator. The optical pulse goes back and forth inside the cavity and overlaps with a fresh electron bunch in each round trip. The radiation is reinforced until the gain equals the total cavity loss. However, because of the different velocities

Received 6 April 2017, Revised 5 July 2017

∗ Supported by National Natural Science Foundation of China (21327901, 11205156)

1) E-mail: liheting@ustc.edu.cn

of the electron beam and optical pulse, the optical pulse gradually advances on the electrons. The slippage length is

$$\Delta S = N_{\mathrm{u}}\lambda_{\mathrm{s}}, \tag{1}$$

where N_{u} is the period number of the undulator, and λ_{s} is the resonant wavelength. The slippage effect induces a longitudinal mismatch, which will be reinforced in each round trip and reduce the saturated power. Therefore, cavity length detuning ΔL is introduced to improve the coupling efficiency. Zero detuning ($\Delta L=0$) is defined as the cold cavity length required to obtain the perfect overlap between the optical pulse and the electron bunch, and a positive value of ΔL means shortening with respect to the ideal cavity length. According to super-mode theory [18], the normalized slippage length μ is defined as

$$\mu = \frac{\Delta S}{\sigma_{\mathrm{e}}}, \tag{2}$$

where σ_{e} is the RMS electron bunch length. The optical field inside the cavity can be considered as consisting of many super modes. The gain of these modes specifies the FEL gain. Without considering the 3D effects, when the small signal gain g_0 is not too large, the total FEL gain $G(g_0,\mu,\theta)$ and optical power $W_{\mathrm{p}}(g_0,\mu,\theta,\eta)$ can be simplified as [19]:

$$G(g_0,\mu,\theta) \approx 1.86 g_0\theta[1-\ln(2.19\theta+0.72\mu\theta)], \tag{3}$$

$$W_{\mathrm{p}}(g_0,\mu,\theta,\eta) = 2.414\left[\sqrt{\frac{\theta_0}{\theta(1+0.33\mu)}} \times \exp\left[0.5\left(1-\frac{\eta\theta_0}{0.85g_0\theta(1-\eta)}\right)\right]-1\right], \tag{4}$$

where $\theta_0=0.456$, η is the cavity loss, and $\theta=4\Delta L/(g_0\Delta S)$ is the cavity detuning parameter.

Furthermore, if μ is larger than 1, the optical pulse width σ_{p} is approximately proportional to $(|\Delta L|/\sigma_{\mathrm{e}}g_0)^{1/3}$. It is obvious that σ_{p} becomes shorter with the decrease of ΔL. $\Delta L=0$ corresponds to the minimum optical pulse length in the case where the laser lethargy effect is ignored. However, when laser lethargy is included, the minimum pulse length occurs when $\Delta L>0$. In other words, the electron bunch and optical pulse are not perfectly synchronised.

If μ is less than 1, however, due to the trapped-particle instability, a series of sub-pulses are probably generated inside the optical pulse, which is the so-called comb structure [20]. The dependence of σ_{p} on ΔL becomes complicated. Generally speaking, when the cavity detuning is not too large, the width of one single spike is comparable to the coherent length l_{c} and σ_{p} is comparable to σ_{e} in the deep saturation region. The coherent length l_{c} is defined as

$$l_{\mathrm{c}} = \frac{\lambda_{\mathrm{s}}}{4\pi\rho}, \tag{5}$$

where ρ is the FEL Pierce parameter [21].

From the discussion above, μ and θ have a strong impact on the longitudinal pulse profile, while peak power can be tuned by varying θ. Moreover, the comb structure may be observed when μ is less than one, which is associated with the trapped-particle instability, and as such has a duration that is set by the building process in the radiation field. In addition, when the small signal gain g_0 is larger than 0.3, Eqs. (3) and (4) should be modified, as discussed in detail in Ref. [19].

3 Simulations

The middle infrared FELO of FELiChEM covers the spectral range of 2.5–50 μm. Here we take the wavelengths of 5 μm and 50 μm as examples for simulations. The corresponding parameters are listed in Table 1. For the 50 μm and 5 μm cases, the small signal gains g_0 are 0.46 and 0.96, respectively, and the out-coupling rates are calculated to be 5% and 6%, respectively. Based on the super-mode theory, the 1-D detuning curves are given in Fig. 1, which show that the output powers for both wavelengths achieve their maximum values when the detuning is slightly larger than zero, due to the optical pulse travelling slower than the speed of light in vacuum. From Fig. 1, the optimal detunings for maximizing the output power are 6.5 μm and 1.2 μm, respectively.

Table 1. Parameters of the Mid-infrared FELO of FELiChEM for wavelengths of 5 μm and 50 μm.

parameter	specification
radiation wavelength/μm	5, 50
beam energy/MeV	50, 25
beam transverse emittance/μm.rad	30
beam energy spread	0.5%, 1%
rms bunch length/ps	4
bunch charge/nC	1
undulator type	Planar
undulator period/cm	4.6
undulator parameter K	1.47, 2.89
period number	50
cavity length/m	5.04
Rayleigh length/m	0.77
outcoupling hole diameter/mm	1.0, 3.0

Actually, many other factors also influence the output properties, such as the electron beam emittance and so on. Therefore, we numerically study the output characteristics by three-dimension simulations with GENESIS code [22] in combination with OPC code [23]. However, the GENESIS code limits the cavity length detuning only to half-integer multiples of radiation wavelength. With an external script that shifts the temporal position of the electron beam by an arbitrary step with respect to the FEL pulse in each round trip, we are able to detune the cavity length finely.

The cavity detuning curves for FEL pulse energy based on 3-D simulation are shown in Fig. 2. The curves have almost the same shapes as those depicted in Fig. 1. The optimal detuning length ΔL_{op} is defined by the maximum energy. Thus ΔL_{op} for the two wavelengths are 25 μm and 5 μm respectively, which are approximately 4 times bigger than those from 1-D analysis. In reality, specific detuning then acquiring of optimal output characteristics should be based on experiments.

With the optimal cavity length detuning, the evolution of output pulse energy is shown in Fig. 3. The pulse energies increase rapidly in the first 50 round trips and saturate at 320 μJ and 240 μJ, respectively.

For the 50 μm wavelength case, Fig. 4 shows the corresponding temporal and spectral structures of the optical pulse at saturation with different cavity length detuning. The results indicate that: 1) When ΔL<25 μm, the pulse width decreases and the spectral bandwidth increases with the increase of ΔL; 2) When ΔL>25 μm, the pulse width increases and the spectral bandwidth decreases with the increase of ΔL.

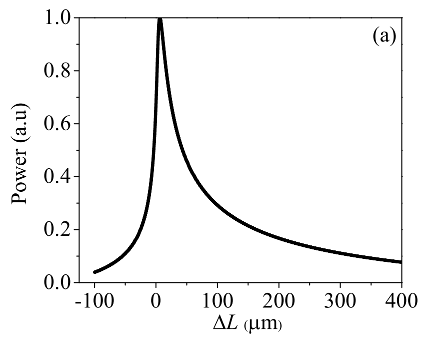

Fig. 1. 1-D detuning curves of the cavity length for radiation wavelengths of (a) 50 μm and (b) 5μm.

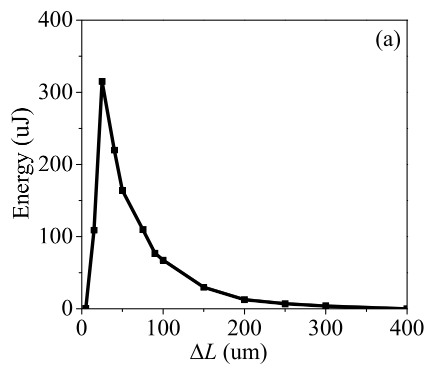

Fig. 2. 3-D detuning curves of the cavity length for radiation wavelengths of (a) 50 μm and (b) 5 μm.

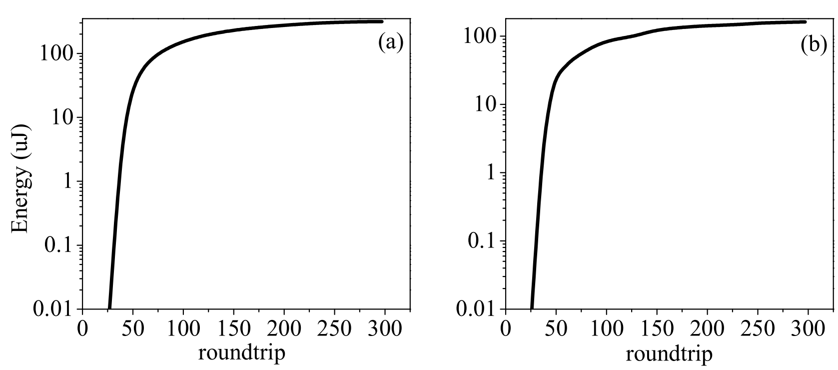

Fig. 3. Evolution of micropulse energy for radiation wavelengths of (a) 50 μm and (b) 5 μm, with optimal cavity length detuning of 25 μm and 5 μm, respectively.

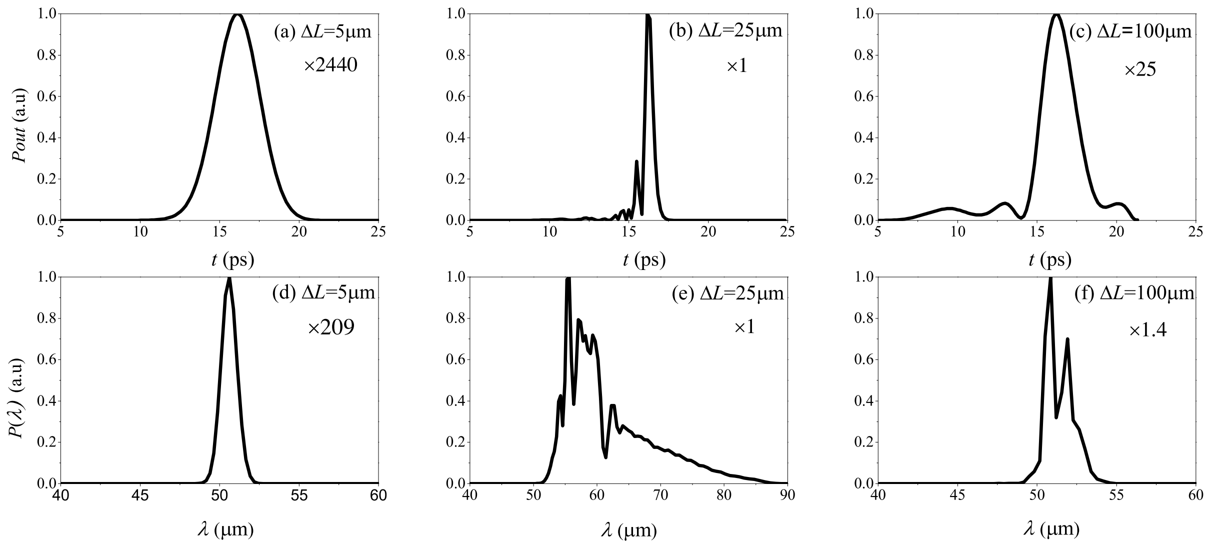

Fig. 4. Temporal and spectral structures of the FEL pulses at saturation with different detuning, for a wavelength of 50 μm. Both the intensity values are normalized to those of ΔL=25 μm.

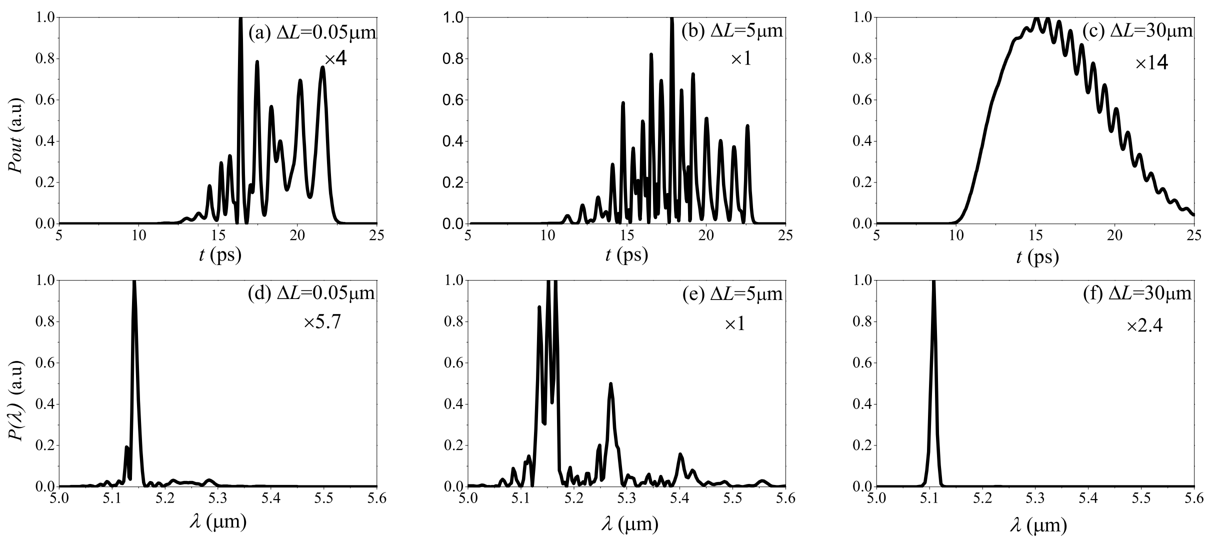

Fig. 5. Temporal and spectral structures of the FEL pulses at saturation with different detuning, for a wavelength of 5 μm. Both the intensity values are normalized to those of ΔL=5 μm.

In our simulations, the optimal detuning ΔL_{op} corresponds to the narrowest pulse width and the widest spectral bandwidth, which is consistent with the analysis of super-mode theory in Section 2 and was first proposed in Ref. [19]. From these results, the pulse width can be tuned in the range of 1–3.2 ps with corresponding RMS bandwidth 13%–1% by adjusting ΔL from 5 μm to 100 μm.

The temporal and spectral structures at saturation with different detuning for the 5 μm wavelength are given in Fig. 5. The pulse RMS width can be tuned in the range of 3.2–6 ps with corresponding spectral width of 2%–0.2% when adjusting ΔL from 0.05 μm to 30 μm. At this time, a comb structure is generated inside the optical pulse, with a single spike width approximately comparable to the coherence length l_{c} and the pulse width σ_{p} comparable to the electron bunch length σ_{e} for optimal detuning. Furthermore, the pulse width dependence on ΔL has no obvious change in the deep saturated region, such as in Fig. 5(a) and (b). Such behavior was predicted in Ref. [24] and has been experimentally observed in several FELO groups [25, 26].

4 Analysis of the comb structure

The super-mode theory and simulation results indicate that the normalized slippage length μ has a distinct influence on the output characteristics. After experiencing enough setting-up time for the optical field, the comb structure may emerge gradually.

Firstly, for the 5 μm case, μ is equal to 0.2 (μ<1). With the optimal cavity detuning length (small ΔL), as shown in Fig. 6, the comb structure starts to emerge at the 50th roundtrip when the power is near saturated. The optical pulse duration also grows gradually with the increase of oscillation number. In the deep saturated region, the width of a single spike is approximately comparable to the coherence length l_c, which is calculated by Eq. (5) to be 130 μm. Moreover, from Fig. 5(c), when $\Delta L = 30$ μm, the output power is small and the comb structure is less likely to occur. Simulation results not shown here indicate that the comb structure will disappear when the cavity length detuning is larger. As ΔL decreases in some degree, the improved coupling between electrons and optical pulse generates higher power, and the comb structure inside the pulse appears. In this case, the comb structure first appears at the head of the optical pulse, then moves towards the tail. At small ΔL, the output power is large enough to make a rich comb structure occur.

Secondly, for the 50 μm case, μ is equal to 2 (μ>1). There is almost a single spike inside the optical pulse in Fig. 4. In order to further verify the influence of μ on the comb structure, we make σ_e 2 and 4 times bigger than before and keep other parameters constant for the 50 μm case, namely, μ is 2, 1 and 0.5. With the optimal detuning, the corresponding optical pulse structures are shown in Fig. 7.

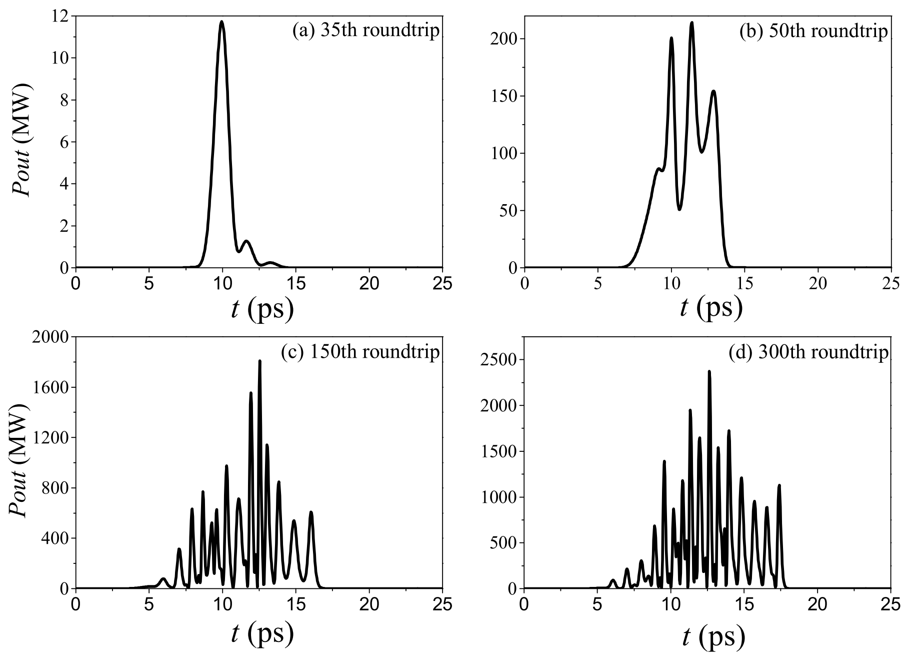

Fig. 6. Evolution of the temporal structure at different roundtrips for the wavelength of 5 μm. The cavity length detuning is 5 μm.

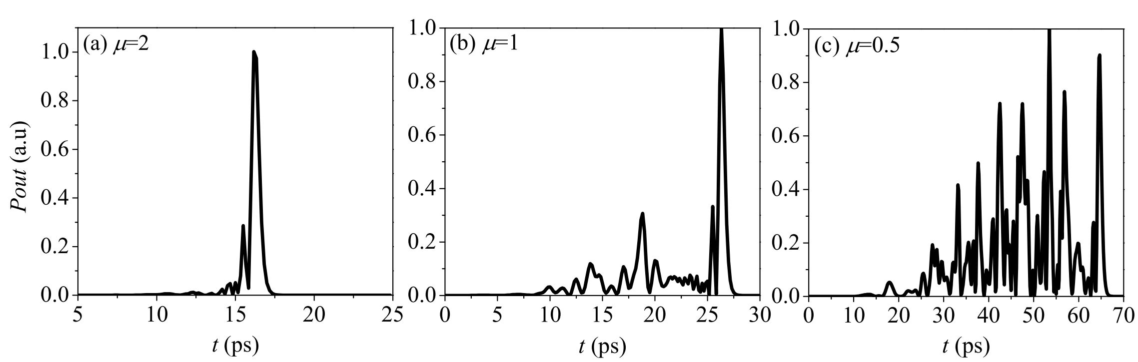

Fig. 7. Relationship between μ and comb structure inside a pulse in the deeply saturated region for the 50 μm case with optimal detuning.

The differences in the 5 μm and 50 μm cases imply that μ plays an important role in the emergence of comb structure. When μ is big enough, the comb structure phenomenon is not apparent; when μ becomes smaller, especially smaller than one, the comb structure phenomenon is remarkable in the deep saturation region and each single spike width is comparable to l_c. The corresponding width of the optical pulse is comparable to σ_e. Furthermore, the FELO output power should be big enough to make the comb structure come out.

5 Conclusions

In this paper, we have numerically studied the output characteristics of the mid-infrared FELO of FELiChEM with cavity length detuning. The results show that the cavity length detuning has a significant impact on the power, temporal and spectral structures of the output FEL pulse. The output pulse duration can be tuned in the range of 1–6 ps with corresponding bandwidth of 13%–0.2% by adjusting the cavity length detuning. Furthermore, the special discussion on the comb structure proves that it occurs in the deep saturation region when the normalized slippage length is less than unity. The comb structure, i.e., mode-locked structure, has been widely studied in high-gain FELs. This paper indicates the possibility of implementing natural mode-locking with conventional FEL oscillators. On the other hand, if not desired, it can be avoided by operating the oscillator with a relatively large detuning length. This work will provide theoretical support for the operation of the mid-infrared FELO of FELiChEM and other similar facilities.

References

1 P. Emma et al, Nat. Photon., **4**: 641 (2010)
2 E. Allaria et al, J. Synchrotron Rad., **22**: 485 (2015)
3 DENG Hai-Xiao et al, Chinese Physics C, **38**: 028101 (2014)
4 J. M. Ortega, Nucl. Instrum. Methods A, **341**: 138 (1994)
5 N. Vinokurov, J. of IRMM&THz Waves, **32**: 1123 (2011)
6 L. Giannessi et al, Phys. Rev. Lett., **106.14**: 144801 (2011)
7 Z. T. Zhao et al, Nature Photonics, **6**(6): 360-363 (2012)
8 J. M. Ortega, M. Bergher, R. Chaput et al, Nucl. Instrum. Methods A, **285**: 97-103 (1989)
9 W. Schollkopf et al, First lasing of the IR FEL at the FritzHaber Institut, Berlin. Proc. of FEL Conference. Nara, Japan. 2012, p. 1-4
10 W. Schollkopf et al, The new IR and THz FEL Facility at the Fritz Haber Institute in Berlin. Proc. of SPIE, **9512**: 95121L-1 (2015)
11 P. W. van Amersfoort, R. W. B. Best, R. van Buuren et al, Nucl. Instrum. Methods A, **296**: 217-221 (1990)
12 P. W. van Amersfoort, R. J. Bakker, J. B. Bekkers et al, Nucl. Instrum. Methods A, **318**: 42-46 (1992)
13 Heting Li, Yalin Lu, Zhigang He, Qika Jia, and Lin Wang, J. of IRMM&THz Waves, **37**: 649-657 (2016)
14 Y.-C. Huang, Appl. Phys. Lett., **96**: 2315039 (2010)
15 He-Ting Li, Qi-Ka Jia, Shan-Cai Zhang, Lin Wang, and Yong-Liang Yang, Chinese Physics C, **41**: 018102 (2017)
16 Kim, Kwang-Je, Phys. Rev. Lett., **66**: 2746 (1991)
17 N. Piovella et al, Physical Review E, **52**(5): 5470 (1995)
18 G. Dattoli et al, IEEE J. Quantum Electron, **17**: 1371 (1981)
19 G. Dattoli et al, Journal of Applied Physics, **101**: 103109 (2007)
20 P. L. Ottaviani et al, Nucl. Instrum. Methods A, **834**: 108-117 (2016)
21 R. Bonifacio et al, J. of IRMM&THz Waves, **28**(9): 699-704 (2007)
22 S. Reiche, Nucl. Instrum. Methods A, **429**: 243 (1999)
23 Vander slot P et al, Phys. Rev. Lett., **102**: 244802 (2009)
24 W. B. Colson, Nucl. Instrum. Methods A, **250**: 168-175 (1986)
25 B. A. Richman, J. M. J. Madey, E. Szamers, Phys. Rev. Lett., **16**: 1682 (1989)
26 G. M. H. Knippels et al, Phys. Rev. Lett., **75**: 1755 (1995)